Intestinal Availability and Metabolic Effects of Dietary Camelina Sphingolipids during the Metabolic Syndrome Onset in Mice

Dominique Hermier, Annaig Lan, Frederique Tellier, Anne Blais, Marta Culetto, Veronique Mathe, Yannick Bellec, Lionel Gissot, Philippe Schmidely, Jean-Denis Faure

???availability and metabolic effects of dietary camelina sphingolipids during the metabolic syndrome onset in mice.

Dominique Hermier[1] *, Annaïg Lan[1], Frédérique Tellier[2], Anne Blais[1], Marta Grauso Culetto[1] Véronique Mathé[1], Yannick Bellec[2], Lionel Gissot[2], Philippe Schmidely[3], Jean-Denis Faure[2].

[1], UMR Physiologie de la Nutrition et du Comportement Alimentaire, AgroParisTech, INRA, Université Paris-Saclay, 75005, Paris, France

[2], Institut Jean-Pierre Bourgin, INRA, AgroParisTech, CNRS, Université Paris-Saclay, 78000, Versailles, France

[3], UMR Modélisation systémique Appliquée aux Ruminants, AgroParisTech, INRA, Université Paris-Saclay, 75005, Paris, France

*, corresponding author:

Dominique Hermier, UMR Physiologie de la Nutrition et du Comportement Alimentaire, AgroParisTech, 16 rue Claude Bernard, F-75005 Paris, France

Phone : 33(1)44087246

Fax: (33)144081858

Email: dominique.hermier@agroparistech.fr

ABSTRACT.

Sphingolipids appear as a promising class of components susceptible to prevent the onset of the metabolic syndrome (MetS). Gut availability and effects of *Camelina sativa* sphingolipids were investigated in a mouse model of dietary-induced metabolic syndrome. Seed meals from two *Camelina sativa* lines enriched respectively in C24- and C16- NH_2-glycosyl-inositol-phosphoryl-ceramides (NH_2GIPC) were used in hypercaloric diets. After 5 weeks on these two hypercaloric diets, two markers of the MetS were alleviated (adiposity and insulin resistance) as well as inflammation markers and colon barrier dysfunction. A more pronounced effect was observed with the C16-NH_2GIPC-enriched HC diet, in particular for colon barrier function. Despite a lower digestibility, C16-NH_2GIPC were more prevalent in the intestine wall. Sphingolipids provided as camelina meal can therefore counteract some deleterious effects of a hypercaloric diet in mice at the intestinal and systemic levels. Interestingly, these beneficial effects seem partly dependent on sphingolipid acyl chain length.

Key words: sphingolipid, *Camelina sativa*, metabolic syndrome, digestibility, acyl chain.

INTRODUCTION

The metabolic syndrome (MetS) is a cluster of abnormalities including visceral obesity, dyslipidemia, hyperglycemia, and increased blood pressure, which results in a higher risk of cardiovascular diseases and type-2 diabetes [1].

Its prevalence is increasing worldwide and makes it a major public health challenge. This increase is associated with several features of lifestyle such as physical inactivity, psychosocial stress, environmental contaminants, and, as a major determinant, dietary habits [2]. High caloric intake, typical of Western-type diet rich in saturated fatty acids (SFA) and sugars, is a major causative factor of the onset of the MetS, which is characterized by early events such insulin resistance (IR) and a low-grade inflammation (LGI) [3, 4]. These alterations are known to originate, at least partly, from an allostatic stress due to the Western-type diet, which is characterized by microbial dysbiosis [5], together with local inflammation [6] and physiological dysfunction of the intestinal wall [3]. The resulting endotoxemia enhances the low-grade inflammation (LGI) at the systemic level, which, in turn, amplifies the initiation of the MetS [7, 8] In addition to the rodent studies, both observation and intervention human studies confirmed the link between nutrients, gut dysfunction, LGI and initiation of the MetS, and in particular IR [8, 9].

In consequence, new preventive and therapeutic strategies for MetS, including lifestyle-based changes involving nutrition, must be established, tested and improved in specifically susceptible and vulnerable people, such as the at-risk, obese subjects. In these patients, the challenge is to prevent or delay the onset of IR and low-grade inflammation, and of cardio-metabolic complications. Among the different possible solutions are diet changes and/or diet complementation.

As part of dietary candidates susceptible to prevent or alleviate the onset of the MetS, and

particularly of IR, sphingolipids (SL) appear as a new and promising class of components. Indeed, body SL originate from endogenous synthesis, but may also be provided by the diet from animal or vegetal products. SL are composed of a sphingoid base (or long-chain base, LCB) acylated by a long or very long-chain FA and bearing a more or less complex polar head group [10]. They are essential components of cell membranes and are involved in cell signalling in both plants and animals. They are associated, together with animal cholesterol or plant phytosterols, into membrane micro-domains (caveolae and lipid rafts) [11]. These micro-domains are more ordered and less fluid than the rest of the plasma membrane, which favours docking, clustering and functionality of insulin receptor and other membrane receptors [11, 12]. Interestingly, the length of the SL acyl chain is an important structural feature modulating the properties of these micro-domains and subsequent translocation and downstream signalling of insulin receptor [13]. A number of disparate, but convincing data, suggest that some plant SL (phytoSL) would improve some features of the MetS, such as dyslipidemia [14, 15], IR/glucose intolerance [15-18] and non-alcoholic steatohepatitis [14, 18-20]. There is also some evidence that dietary SL from both animal and plant origin may exert anti-inflammatory effects at the extra-digestive level, including in the postprandial state [21, 22].

Other beneficial effects of phytoSL have been described at the intestine level, in mice models of chemically-induced colorectal cancer or inflammatory bowel diseases [23-28]. In contrast, when it comes to nutritionally-induced rather than chemically-induced, allostatic intestinal stress, it remains unknown if dietary phytoSL may alleviate microbial dysbiosis and/of gut barrier function alterations, which could explain some beneficial systemic consequences.

The mechanisms by which phytoSL exert their beneficial effects are still not elucidated and

since it is a large and diversified lipid family, the role of the different structural components (polar head, acyl chains, long chain base) remains to be deciphered. Indeed, plants have a large variety of SL with more than 300 molecular species, some of which being tissue specific [29]. They are characterized by specific polar heads like glycosyl-inositol-phosphoryl-ceramides (GIPC) and LCB like phytosphingosine (PHS, t18:1). Seeds also accumulate specific amino-derivate GIPC (NH_2GIPC) [29].

Taken together, available data suggest that plant-derived SL can have beneficial effects on the MetS onset. However, all previous studies were performed by using purified SL and, most often, plant SL were administered orally or intra-peritoneally, and not as diet ingredient. The objective of the present study was therefore to assess (i) whether plant SL provided as part of the diet (i.e. as a food ingredient in a food matrix) could counteract MetS onset and (ii) whether SL acyl chain length is important in modulating the physiological and metabolic impact of dietary phytoSL. Because bioavailability is an essential prerequisite to extra-digestive effects, digestibility of phytoSL with different acyl chain length had also to be determined. Plant SL originating from two isogenic camelina cultivars in which SL were differing only by their fatty acid (FA) chain length were provided as seed meal to mice fed for 5 weeks with high-fat/high sucrose diets. The first outcome was to assess the bioavailability of dietary phytoSL at the digestive level, by using plant sphingolipidomic profiling, and their possible impact on intestinal function. The second one was to evaluate if dietary phytoSL could slower the onset of the MetS, especially as regards dyslipidemia and IR. Finally, the hypothesis that acyl chain length may modulate digestibility and bioactivity of phytoSL was also tested for both the outcomes.

MATERIALS AND METHODS

Selection of C16-SL accumulating camelina line. *Camelina sativa* cultivar "Céline" was grown in glasshouse conditions as described previously [30]. To generate plants accumulating SL rich in C16 FA (C16-SL) , the coding sequence of the Arabidopsis ceramide synthase AtLOH2 (At3g19260) was PCR amplified using LOH2EcoRI-F and LOH2XhoI-R primers modified with EcoRI and XhoI restriction enzymes (LOH2EcoRI-F, GGAATTCATGGAATCGGTATCATCACG; LOH2XhoI-R, CCGCTCGAGCTAATCATCATCATCCTCTG) and cloned behind the soybean glycinin promoter into the pBinGlyRed2 vectors after removal of the Luciferase coding sequence using the EcoRI/XhoI enzymes. Plants were transformed by flower dip infiltration with *Agrobacterium tumefasciens* carrying pBinGlyRed2::AtLOH2 and T1 seeds were selected based on their red fluorescence [31]. A total of 107 T2 progeny were produced and screened for their respective seed SL content by LC-MS/MS. Eight T3 progeny were eventually selected and amplified and rescreened for their seed SL content. A homozygous line named LOH2^{Y} with the highest C16-SL content was finally selected and amplified as T4 and T5 generations. Complete SL profile was carried out on T5 seeds, as described below.

A total of 1476 wild type camelina and 1593 LOH2^{Y} T4 plants were cultivated side by side in the glasshouse, resulting in the production of 6.1 kg of Céline seeds (of which SL-FA are mostly C24) and 5.4 kg of T5 LOH2^{Y} seeds (rich in C16-SL). Camelina seeds were crushed with an Oilprinz KK8 F universal (Kern Kraft, Reut, Germany) at 60 rpm and with opening of 8 mm to produce CamC24 and CamC16 meal and oil from Céline and LOH2^{Y} seeds respectively. Macronutriment composition of the camelina meal was determined as previously described [32] and was (in weight %): 36.5/39.4 protein, 19.7/19.8 lipid, 29.4/28.8 fibre, 5.79/5.83 ashes and 5.70/5.81 humidity for the CamC24 and CamC16, respectively. Fibre typology was the same in both meals (data not shown).

Animals and diets. Thirty-three 7-week old male C57BL/6JOlaHSD mice (Envigo, Gannat, France) were housed in individual cages with wired floor, at 22 ± 1°C under 12-h light/dark cycles (light on at 07:00 am) and acclimated to local conditions for 1 week. During the last 3 days of the week, 27 mice were progressively switched from the standard pelleted chow diet (SAFE A04, Augy, France) to the control hypercaloric (HC-Con) diet (see below). At 8 weeks of age, mice were divided into 4 groups and fed during 5 weeks with either the same chow diet as before (normocaloric diet, NC group, n=6) or one of the three hypercaloric (HC) diets, two providing one of the two camelina meals (HC-CamC24 and HC-CamC16, n=9) and the third one a control HC diet (HC-Con n=9) (**Supplemental Table 1**). Mice had free access to food and tap water. Individual body weight was recorded weekly. The study was performed according to the European directive for the use and care of laboratory animals (2010/63/UE), and received the agreement of the local animal ethics committee and of the ministerial committee for animal experimentation (Ref 20151I0317422745.v4-APAFIS#2701).

HC diets were prepared freshly twice a week, stored at 4°C, and provided daily to mice as soft pellets. CamC24 and CamC16 meals from the commercial Céline cultivar and LOH2^{Y} line were incorporated into the HC diets (respectively HC-CamC24 and HC-CamC16). Camelina oil obtained from Céline seed crushing was kept at 4°C and incorporated into the HC-Con diet at the same level as in the two HC-CamC24 and HC-CamC16 diets. It contains as previously described mostly polyunsaturated FA (53%) and monounsaturated FA (29%), as previously described [31]. SL analysis of this oil showed the absence of NH_2GIPC, the major SL in both camelina meals.

Sphingolipid were extracted from camelina meals, oils and diets, as described previously [29]. CamC24 and CamC16 meals contained the same levels (in nmol/g) of total phytoSL and

158 NH_2GIPC, which was the major SL in both meals (92%) (**Supplemental Table 2**). In contrast,
159 C24-NH_2GIPC accounted for 82% of total NH_2GIPC in CamC24, whereas C16-NH_2GIPC
160 accounted for 90% of total NH_2GIPC in CamC16. The amount of camelina meals to be
161 incorporated into the HC-CamC24 and HC-CamC16 diets (107g/kg) was calculated according
162 to the SL content of the camelina meals, the mice food intake (about 4 g/d for a HC diet) and
163 the amount of purified plant SL given to rodents in the literature (4-8 mg/d in mice, without
164 indication of their body weight) [14, 16]. SL profile of the HC-CamC24 and HC-CamC16 diets
165 reflected that of the respective meals, with NH_2GIPC being the major SL with mostly by 24
166 carbons FA in CamC24 meal, and by 16 carbons FA in CamC16 meal (**Table 1**). As expected,
167 HC-Con diet contained very little NH_2GIPC, whereas the NC diet was surprisingly rich in SL,
168 and especially in NH_2GIPC, probably as a consequence of the high level of plant-based
169 materials (e.g. soya bean) in the commercial chow.
170
171 ***In vivo* measurements and sample collection.** Food intake during 48 h was monitored after
172 6 d and 4 wk on the experimental diets. Feces were collected and weighed for further
173 lipidomics at the end of the 48 h. Part of the feces was freeze-dried before assaying the dry
174 matter content [32]. Apparent digestibility of the dry matter was calculated as follows:
175 (intake-feces content)/intake*100. SL apparent digestibility was calculated by applying the
176 same formula to SL content measured in food and feces.
177 The body composition (fat mass and lean mass) was measured *in vivo* after 3 weeks on
178 the experimental diets by dual energy X-ray absorptiometry (DEXA), using a Lunar PIXImus
179 densitometer (GE Medical Systems, Buc, France). The stability of the device was controlled
180 by a measurement of a phantom before each session. The mice were anesthetized by
181 isoflurane inhalation during the measurement. Analysis of the images was performed with

182 the software provided with the device (Lunar PIXImus v2.10, GE Medical Systems, Buc,
183 France), using auto-thresholding.

184 An oral glucose tolerance test (OGTT) was performed after 3 weeks on the experimental
185 diets. Six hours fasted mice were weighed and a blood sample (~25 µL) was taken from the
186 tail vein ~15 min before (t0) gavage, then after 15, 30, 60, and 120 min following orally
187 administration of a glucose solution (2 g/kg). Blood glucose concentration was immediately
188 assayed using a standard glucometer (Onetouch, LifeScan, Boulogne-Billancourt, France).
189 Blood was centrifuged (10 min, 1600 *g*, 4°C) and plasma stored at -20°C for subsequent
190 assay of insulin.

191 After 5 weeks on the experimental diets, mice were fasted for 6 h. After a blood sample
192 has been taken from the tail vein for glucose determination, mice were deeply anesthetized
193 by isoflurane inhalation (IsoFlo, Axience, Pantin, France). Blood was taken by cardiac
194 puncture before mice were euthanized by exsanguination. The abdominal cavity was then
195 opened and the following parts were removed and weighed: liver, epididymal adipose
196 tissue (EpAT), kidneys, spleen, small intestine, caecum and colon. The luminal contents of
197 the caecum and the colon were removed and weighed. Jejunum, colon and EpAT samples
198 were snap-frozen in liquid nitrogen and stored at -80°C. Blood samples were centrifuged as
199 described above for plasma extraction and storage.

200

201 ***Ex vivo* intestinal measurements.** To assess potential changes in intestinal barrier function,
202 electrophysiological measurements were performed as previously described [(33)] with the
203 following modifications: each mouse proximal colon was opened along the mesenteric line
204 and mounted on an EasyMount Ussing chamber insert (Physiologic Instrument Inc, San
205 Diego, CA, USA) with an exposed area of 0.2 cm^2. Mounted tissues were left to equilibrate

206 their trans-epithelial potential (V_t, mV) 45 min before clamping them to 0 mV to obtain the
207 short-circuit current (I_{sc}, µA/cm^2). The trans-epithelial electrical conductance (G_t, mS/cm^2)
208 was obtained using the Ohm law by the voltage deviation when the tissue was current
209 pulsed with ± 5 µA.
210 Paracellular permeability to fluorescein isothiocyanate (FITC)-dextran 4000 (FD4, Sigma) was
211 determined during a 100-min period in Ussing chambers. Soon after tissue mounting (t_0),
212 FD4 was added to the chamber mucosal side at the final concentration of 0.250 mg/mL.
213 Serosal samples were collected at t_0 and after 100 min. To test for tissue viability at the end
214 of the experiment, carbachol (CCh, 10^{-4} M) was applied at the serosal side verifying the
215 activation of the calcium-dependent chloride secretion by the I_{sc} increase.
216
217 **Biochemical analyses and physiological measurements.** Blood glucose concentration was
218 determined with an Accu-Chek® glucometer (Roche Diagnostics, Meylan, France). Plasma
219 triglyceride concentrations were determined by colorimetric enzymatic methods using a
220 commercial kit adapted for use in a 96-well microplate reader (Molecular Devices, Saint-
221 Grégoire, France), and obtained from Randox (Roissy, France) [34, 35]. Plasma insulin was
222 determined using enzyme-linked immuno-assay (Mouse insulin ELISA, Mercodia, Paris,
223 France). Homeostasis model assessement of insulin resistance (HOMA-IR) index was
224 calculated using the formula: [fasting insulin (pmol/L) x fasting glucose (mmol/L)]/22.5.
225
226 **Sphingolipidomics.** SL were extracted from feces, jejunum and colon as described previously
227 [36]. A volume of 500 µL isopropanol:hexane:water (55:20:25, v/v) and 10 µL standard mix
228 [0.01 nmol of C12-Cer (d18:1-h12:0), 0.1 nmol of C12-GluCer (d18:1-h12:0) and 0.2 nmol of
229 ganglioside (GM1)] were added to material and ground using a Polytron homogenizer. The

plunger was rinsed with 500 µL of extraction solvent and the sample incubated at 60°C for 15 min. After centrifugation at 4000 rpm for 5 min at room temperature, the supernatant was recovered and the pellet extracted once more with 1 mL of solvent. Supernatants were combined and dried with a speed Vac. Then the samples were incubated at 50°C for 1 h with 500 µL of 33% methylamine solution in ethanol-water (7:3) and dried under nitrogen and resuspended by sonication in 100 µL of tetrahydrofuran-methanol-water (2:1:2) containing 0.1% formic acid and filtrated prior to analysis by liquid chromatography coupled to mass spectrometry (UPLC- MS/MS). UPLC- MS/MS analyses were carried out on a Waters Acquity UPLC system coupled to a Waters Xevo tandem quadrupole mass spectrometer equipped with an ESI source (Waters, Milford, MA, USA). Chromatographic conditions, mass spectrometric parameters, and multiple reaction monitoring (MRM) methods were defined as described previously [29].

Gene expression. Total RNA was extracted from EAT and colon samples using Trizol reagent (Invitrogen, Carlsbad, CA, USA). qRT-PCR was performed with mouse-specific primers (Eurogentec, Angers, France) to quantify mRNA level of the following genes : interleukin-6 (*Il-6*), interleukin-1β (*Il-1β*) interleukin-10 (*Il-10)* and tumor necrosis factor-α (*Tnf-α)* in both EAT and colon, plasminogen activator inhibitor-1 (*Pai-1) and* monocyte chemoattractant protein-1 (*Mcp-1*) in EAT, and claudin 1 (*Cldn1)* and zonula occludens (*Tjp1*) in the colon. After cDNA synthesis from mRNA using High Capacity cDNA Reverse Transcription Kit (ThermoFisher-Life Technologies, Les Ulis, France), Real-Time PCR was performed subsequently on cDNA using the power SYBR Green PCR master mix and StepOne Real-Time PCR system (ThermoFisher-Life Technologies, Les Ulis, France). cDNA samples were assayed

in triplicate and gene expression levels for each sample were normalized relative to hypoxanthine-guanine phosphoribosyltransferase gene (*Hprt*) with $2^{-\Delta\Delta Ct}$ calculation.

Statistical analyses. Data are reported as means ± standard deviations. They were analysed using the XLSTAT application (Addinsoft, Paris, France). Significance level was set at $P<0.05$. The effects of energy level (HC vs NC) and of camelina meal (HC-Con vs HC-CamC16/C24) were tested using a 2-way ANOVA. When diet effect was significant, differences between means were tested for significance using the *post-hoc* Tukey procedure.

RESULTS.

Production of Camelina seeds with different sphingolipid contents. The high expression of the C16 specific Ceramide synthase LOH2 from Arabidopsis in *Camelina sativa* led to seeds with opposite sphingolipid profile (**Supplemental Figure 1**). Camelina seeds and meals (cake fraction from seeds) from commercial cultivar Céline (CamC24) presented characteristic sphingolipid profile with high levels of NH_2GIPC almost exclusively with very long chain FA (C24). Conversely, the LOH2 expressing line LOH2^{Y} (CamC16) accumulated almost exclusively C16 NH_2GIPC albeit the levels of total sphingolipids remained similar to CamC24. C16 GluCer was also increased and C24 GluCer strongly decreased in CamC16 (**Supplemental Table 2**). A similar trend was also observed for Cer and hCer but at a much lower scale. The most abundant LCB in seeds were t18:0 and t18:1 in both lines even if d18:1 and d18:0 were increased in LOH2^{Y} due to the accumulation of C16 NH_2GIPC and GluCer .The accumulation of C16 SL had a weak impact on plant fitness with a slight delay of germination and slower early growth rate as well as a lower seed yield and weight for LOH2^{Y} (data not shown).

Body weight and associated parameters. During the 5 wk of MetS induction, all mice gained weight, but to a different extent (**Figure 1**). After 5 wk on the experimental diets, mice on the HC-Con diet exhibited a higher weight gain (8.8±1.2g) than mice of the NC group, which gained 3.5±1.1 g only (**Supplemental Table 3**). In both HC-Cam groups, body weight gain, as well as body weight after 2, 3 and 5 weeks on their respective diets, did not differ significantly from the NC group, but were significantly lower than in the HC-Con group (**Figure 1 and Supplemental Table 3**). Food intake (as kcal/d) tended to parallel body weight, and was the highest in the HC-Con group after 6 d and 4 wk, whereas there was no difference between groups at both times when energy intake was adjusted for body weight (**Supplemental Table 3**). Apparent digestibility (% intake of dry matter that was not found in feces) was equivalent after 6 d or 4 wk on the same experimental diets. After 6 d, it was the lowest in the NC group, intermediary in the HC-Con group and the highest in the HC-CamC24 and HC-CamC16 groups, whereas after 4 wk, it remained the highest in the HC-CamC24 group only (**Supplemental Table 3**).

Body composition. After 3 wk on the experimental diets, the lean mass was the same in all groups, whereas the fat mass (absolute and relative to body weight) was as expected higher in the three HC groups than in the NC group, without significant effect of the camelina meals (**Table 2**). After 5 wk, mice of the HC-Con group were significantly heavier than those of the NC group whereas mice of both HC-Cam groups showed intermediate body weight (**Figure 1** and **Table 2**). Similarly, when compared to the NC group, adiposity (absolute and relative weight of the EAT) was globally increased in the three HC groups, but to a lower extent in the HC-Cam groups. While liver and small intestine weights were similar in all groups, the

300 weights of the caecum and the colon, as well as of the caecum content, were significantly
301 lower in the three HC groups.
302
303 **Blood and tissue markers associated with the MetS.** During an OGTT after 3 weeks on the
304 experimental diets, glucose and insulin plasma concentration increased sharply during 15
305 min, then returned to fasting values after 120 min in all groups (**Figure 2**). When compared
306 to the NC group, the HC-Con group exhibited higher fasting glucose and insulin
307 concentration (t0) and AUC over 120 min, as well as higher HOMA-IR index (**Table 3 and**
308 **Figure 2**). Besides, the increase in glucose concentration between t0 and t30 min, which
309 takes into account the difference in fasting glycemia between groups (Δ glucose), was two-
310 fold higher in the HC-Con group than in the NC group. In both HC-Cam groups, fasting
311 glucose concentration and AUC over 120 min were similar to those of the HC-Con group, and
312 higher than in the NC-Con group, whereas insulin AUC and HOMA did not differ from the NC-
313 Con group and were therefore lower than in the HC-group. Interestingly, insulin fasting
314 plasma concentration in HC-CamC16 mice did not differ from the NC mice and was
315 significantly lower than in the HC-Con mice, which was not the case in mice HC-CamC24
316 mice. In the two HC-Cam groups, Δ glucose between t30 and t0 of the OGTT was
317 intermediary between NC- and HC-Con groups.
318 At the end of the experiment, after 5 weeks on the experimental diets, fasting glucose
319 concentrations did not differ from those after 3 weeks, remaining higher in the three HC
320 groups than in the NC group (**Table 3**). Fasting triglyceridemia was identical in NC- and HC-
321 Con groups, but was surprisingly 2-fold lower in the 2 HC-Cam groups. Compared to the NC-
322 Con group, fasting cholesterolemia was higher in all the HC groups but only significantly in
323 both HC-Cam groups.

Transcript levels of a few inflammatory and vascular markers were higher in mice fed the HC diets: *Mcp-1* and *Pai-1* in the adipose tissue (P = 0.011 and 0.002, respectively) and *Il-1 β* in the colon (P = 0.039). However, according to the *post-hoc* Tukey test, and as compared to the NC group, *Mcp-1* and *Il-1β* mRNA levels were significantly higher in the HC-Con group only, and *Pai-1* in the HC-Cam groups only (**Table 4**). Other mRNA levels of inflammatory markers (*Il-6, Il-1ϐ*, *Il-10 and Tnf-α* in the adipose tissue and *Il-6, Il-10, Tnf-α in the colon)* did not differ between groups, neither did those of the tight junction protein encoding genes *Tjp1* and *Cldn1* in the colon (data not shown).

Colon epithelial barrier and permeability. Measurement of electrical parameters in Ussing chambers was performed on proximal colon (**Table 5**). There was no difference in the FD4 permeability within the diet groups, which indicated that paracellular pathway of the gut barrier function in the colon was not altered (data not shown). The colon transepithelial voltage (V_t), which is usually negative at the colonocyte luminal side, was more negative in the 3 HC groups than in the control NC group, this effect being significantly less pronounced in the HC-CamC16 group. Conversely, the short-circuit current (I_{sc}) was higher in the three HC groups, with no difference between them. Trans-epithelial conductance (G_t) in the three HC groups did not differ from that in the NC group, however the HC-CamC16 and the HC-Cam24 groups showed the highest and lowest values respectively.

SL intake, excretion and tissue profile. Apparent NH_2GIPC digestibility (**Table 6**) was calculated after 4 wk of experimental diets, using the *in vivo* measurement of food intake and fecal excretion and the analysis of complete plant sphingolipidomic profiles of diets (**Table 1**) and feces (data not shown). Since NH_2GIPC accounted for nearly 80% of total SL in

348 HC-CamC16 and HC-Cam24 diets, intake and excretion were calculated in this fraction only.
349 Mean individual NH_2GIPC dietary intake, expressed as absolute amounts, grossly reflected
350 their dietary profile. It was very low in the HC-Con group, much higher in the NC group (over
351 40 fold increase), and even further increased in both HC-Cam groups by over 80 fold, with no
352 significant difference between the two groups. In contrast, NH_2GIPC excretion differed
353 markedly between the HC-Cam groups. Excretion rate of NH_2GIPC in the HC-CamC16 group
354 was 2.5-fold higher than that in the HC-CamC24 group. Consequentely, the apparent
355 digestibility of dietary NH_2GIPC was significantly lower (80%) in the HC-CamC16 than in the
356 three other groups (87-94%).
357 Concentration of the most abundant plant SL (NH_2GIPC and GluCer with C16 and C24 FA)
358 was determined in the jejunum and colon walls (**Table 7**). Jejunum and colon of the NC
359 group contained similar amount of C24-NH_2GIPC and C24-GluCer, while the latter was a
360 minor component of the diet. Jejunum and colon of the HC-Con mice were nearly devoid of
361 phytoSL, as expected from their low level in the HC-Con diet. On the contrary, plant NH_2GIPC
362 and GluCer were found in the intestine on mice fed with the camelina meals. As expected
363 C24-SL were the most prominent SL in the HC-CamC24 group, while C16-SL was the most
364 abundant in the HC-CamC16 group, with NH_2GIPC being the most abundant SL in both
365 groups. Tissue content of the various SL species was lower in the colon than in the jejunum,
366 however small levels of plant NH_2GIPC were still present in the colon. Finally, the total
367 concentration of SL (GluCer + NH_2GIPC) in the intestine of HC-CamC16 mice was
368 approximately 2-fold higher in the jejunum (12.5 nmol/g) and in 5-fold higher in the colon
369 (2.14 nmol/g) than in HC-CamC24 mice (6.40 and 0.40 nmol/g in the jejunum and colon,
370 respectively). Interestingly, while C24-GluCer ratio between colon and jejunum was similar in
371 the two HC-Cam groups (0.38 vs 0.41), this ratio was much lower in the HC-Cam24 group

than in the HC-Cam16 group for C24-NH_2GIPC (0.05 vs 0.26) and even lower in the HC-Cam16 group for C16-NH_2GIPC (0.05 vs 0.16).

DISCUSSION.

Digestive bioavailability of camelina SL. In most *in vivo* studies aiming to highlight the mechanisms involved in potentially beneficial effects of plant SL at the systemic level, a dramatic gap remains concerning the bioavailability of plant SL when provided in the diet. Both animal and plant SL are hydrolysed into LCB, FA, and the polar head group in the small intestine, then eventually absorbed, reesterified, and secreted into the lymph [37-40]. As regards phytoSL, it is needed to document to what extent they are digested then absorbed, in which form they are transported and made available to various tissues, and which molecular species are stored in various body compartments.

To our knowledge, the present study quantifies, for the first time, intestinal digestibility of a major phytoSL (NH_2GIPC, accounting for nearly 80% of total SL in the HC-Cam diets) when provided as a dietary component. Camelina NH_2GIPC in the two HC-Cam diets exhibited the same LCB profile, and only differed in their FA length (mainly C24 in the CamC24 meal and C16 in the CamC16 meal). Although apparent digestibility of dietary NH_2GIPC was high, it was lower in the HC-CamC16 group, which could be accounted for by a higher fecal excretion. However, the higher NH_2GIPC content in the gut wall of the HC-Camc16 fed group, suggests some metabolic specificity during reesterification and excretion into the lymph(**Table 7**). Besides, beyond this demonstration of the NH_2GIPC availability at the digestive level, NH_2GIPC-containing SL, or their metabolites, have to be sought in other body compartments, this lack of information being a limitation of the present study.

Effects of the camelina meal on the early markers of the MetS. Plant SL have been shown to exert beneficial effects on some risk factors associated with the MetS, such as altered glucose homeostasis, abnormal lipid profile, and low-grade chronic inflammation. In the present study, we used our mouse model of the early steps of the MetS to explore the effects of dietary plant SL provided by camelina meal in a hypercaloric diet [41]. As expected from this model, after 5 wk on a hypercaloric diet rich in saturated FA and sucrose (HC-Con group), mice exhibited (as compared to those on a normocaloric diet, NC-group) an increase in body weight and adiposity (**Table 2** and **Figure 1**), and in fasting glycemia (**Table 4**). After only 3 wk, these alterations were already detectable and were accompanied by higher values of insulinemia and HOMA-IR index (**Table 3**), and of glucose and insulin postprandial AUC (**Figure 2**). These findings are consistent with data obtained in mice fed a HC diet rich in saturated FA [42].

When SL was provided as camelina meal in the HC diet (HC-CamC24 and -C16 groups), body weight gain and adiposity were reduced, but not the lean mass (**Figure 1** and **Table 2**). This specific effect of camelina meals on adiposity was not accounted for by a lower food intake, since it was the same in all groups after 6 d and 4 wk when normalized for body weight. Whether this effect is due to the presence of SL in the diet is questionable, since no significant effect of phytoSL was reported for body weight, fat mass or body mass index in previous studies [14-17, 43, 44]. In our study, the presence of other components of the camelina meal, such as fibers, may be responsible for a lower nutrient absorption, and subsequent bioavailability, lowering body storage of lipids, either exogenous (dietary) or endogenous (*de novo* synthesised). However, a specific effect of phytoSL may not be precluded, since a very recent study showed that mice fed a high-fat diet supplemented with milk polar lipids containing 25% SL gained less weight than mice on the high-fat diet alone [45].

In parallel, in mice fed by either camelina meal, fasting insulinemia and HOMA-IR index were normalized, as well as insulinemia AUC during an OGTT, and triglyceridemia decreased (**Table 3 and Figure 2**). These findings are grossly consistent with previous studies using purified SL or LCB in rodent mice models exhibiting features of the MetS or in human subjects with a MetS. Indeed, various SL or LCB decreased triglyceridemia in mice or sand rats on a hypercaloric diet [14, 20] whereas phytosphingosine decreased glycemia in subjects with a MetS [15] and improved glucose homeostasis in human subjects with a MetS and various rodent models, [15-19]. In contrast, the present study showed no effect on cholesterolemia, which is inconsistent with previous studies that repeatedly reported a decrease in plasma total, LDL, or non-HDL cholesterol in various rodent models and in subjects with a MetS [14, 15, 17, 20]. One originality of our short-term study is the demonstration that, when focusing on the onset of the MetS, an early alteration of glucose homeostasis, as demonstrated by insulin resistance occurrence both at the fasting state and during an OGTT, may be counteracted by a phytoSL-rich matrix after only 3 weeks on the experimental diets.

The mechanisms by which dietary SL may exert systemic effects remain largely speculative. First, in response to various SL or LCB, a decrease in the postprandial absorption of dietary triglycerides and cholesterol has been suggested, and would explain the downstream effects on lipid metabolism at the hepatic or plasma level [14, 43]. Second, gene regulation by SL or LCB, including activation of various PPARs, and resulting in beneficial effects on insulin sensitivity, glucose tolerance and lipid metabolism have been also demonstrated [17, 20, 43]. Finally, it has been recently shown that animal SL may affect gut microbiota in mice in a way that would limit some detrimental effects of HF diets [45, 46]. All these mechanisms, which remain to be investigated in our model, would contribute to lower adiposity and slower insulin resistance in mice fed the HC-Cam diets (**Table 2**).

444 In response to a diet rich in saturated FA and sucrose, the increased adipose tissue often
445 features an inflammatory phenotype [4]. In the present study that targeted the initial steps of
446 the MetS, there was no evidence that gene expression of pro-inflammatory cytokines was
447 enhanced in the adipose tissue, despite an increased adiposity, and providing SL-rich
448 camelina meal had no significant effect. Gene expression of two others inflammatory
449 markers, *Mcp-1* and *Pai-1*, was enhanced in response to the HC diet (HC-Con group).
450 Attenuation of *Mcp-1* mRNA level may be related to the lower adiposity of mice on both HC-
451 Cam diets, whereas the reason why the HC-Cam diets aggravated the mRNA level of *Pai-1*,
452 remains to be investigated.

453 To our knowledge, the present study, provides the first evidence that a mixture of natural
454 plant SL, essentially in the form of NH_2GIPC, and provided in their original matrix, exerted
455 some beneficial effects during the MetS onset. However, the role of other camelina meal
456 components, such as phospholipids, polyphenols or specific fibers cannot be excluded [47, 48].
457

458 **Effects of the camelina meal on the intestine wall.** When compared to the NC group, the
459 HC-Con diet enhanced a few inflammation markers in the colon and the adipose tissue
460 (**Table 4**). In contrast, in mice fed the camelina meals, mRNA levels of *Mcp-1* in the adipose
461 tissue and of *Il-1β* in the colon did not differ from those in the NC group (**Table 4**). The role
462 of SL in inflammatory processes is still in debate, but a few studies support the hypothesis
463 that dietary phytoSL (as maize GluCer) or animal SL (as sphingomyelin) alleviate gut
464 inflammation in rodent models [23-28]. How plant SL may improve intestinal inflammation
465 remains nonetheless highly speculative. A study using Caco-2 cells suggested that SL may
466 interact with epithelial cells without being absorbed. In these *in vitro* conditions, plant
467 GluCer remained at the cell surface, but decreased LPS-induced production of inflammatory

468 cytokines, maybe by affecting the interactions between LPS and its TLR at the cell surface [28].
469 Similar interactions with non-digested plant SL or their metabolites may contribute *in vivo* to
470 modulate the inflammatory status of the intestine wall. The intestinal microbiota is likely to
471 contribute to these interactions, since it is able to metabolize animal SL, which would
472 contribute to regulate cytokine production [24, 49].

473 Interestingly, epithelial integrity of the colon was specifically modified by the HC-CamC16
474 diet, as demonstrated by its effects on transepithelial voltage (V_t) and epithelial conductance
475 (G_t) (**Table 5**). V_t describes the unidirectional transport of sodium from the luminal to the
476 serosal side of the epithelium. This potential difference is usually negative at the colonocyte
477 luminal side, and was even more negative with HC diets. This effect of HC-diets reflects an
478 increase in the driving force of the colonocytes to allow the sodium, chloride and water
479 absorption from the colon lumen, and therefore a loss of permeability. This decrease in V_t
480 may be related to the high fat content of the diet, known to alter electrical parameters of
481 transcellular barrier function [42, 50, 51]. This damage was attenuated in mice given the diet
482 containing camelina SL rich in C16 FA (HC-CamC16). V_t increase in HC-Camc16 mice was also
483 associated with higher epithelial conductance (G_t) which was not due to a loss of epithelial
484 permeability, at least via the paracellular pathway, because it was not accompanied by an
485 increase in the apical-to-basal flux of the paracellular marker FD4 in any group. The absence
486 of dietary effects on the gene expression of two tight junction proteins, claudin 1 (*Cldn1)* and
487 zonula occludens (*Tjp1*), confirms that the paracellular permeability was not affected by any
488 of the HC diets. Rather, we suggest that, in the colon of the HC-CamC16 mice, this increased
489 G_t may reflect a compensatory mechanism that counteracts the increase of actively
490 transported ions (as evidenced by the higher short-circuit current -I_c- in all HC groups) by
491 increasing passive movement of ions. This would explain the lower value of V_t in the HC-

CamC16 group. Nevertheless, further investigations would be needed to determine the precise mechanisms involved in the action of camelina SL (native or digested products) on activity and/or expression of colon transporters and exchangers that ensured colon barrier integrity and flux. Yet, it can be concluded from the present study than differences in the FA profile of dietary plant SL, and particularly the enrichment of C16 FA in the experimental LOH2^{Y} line (to the detriment of C24 FA in the commercial Céline cultivar) modulate the deleterious effects of a high-fat diet on colon epithelial barrier function, and more specifically on transepithelial permeability.

In conclusion, phytoSL provided in a plant matrix delays the onset of the MetS, by reducing adiposity and insulin resistance. Involved mechanisms at the intestinal and systemic levels remain mostly speculative at this initial stage, but it may be hypothesized that some of the effects observed, including on the adipose tissue and blood parameters, results from an impact of phytoSL or their metabolites at the intestinal level. Moreover, some of these effects are modulated by the FA length of the SL, since they are sometimes more pronounced in presence of C16-NH_2GIPC. More researchs are required to uncover the importance of FA length in the interactions between phytoSL, the intestinal wall, and systemic effects. In this context, interactions of phytoSL and their metabolites with the microbiota may be a promising avenue of investigation.

Acknowledgements

The authors acknowledge the valuable contribution of Célia Carbonne, MSc student in UMR Physiologie de la Nutrition et du Comportement Alimentaire (PNCA), who contributed to the running of the study, and of Morgane Dufay (UMR PNCA) for animal care and help with

516 dissection and sampling. They thank Ophélie Dhumez (UMR Modélisation systémique
517 Appliquée aux Ruminants) for the determination of nutrient composition of the camelina
518 meals.

519

520 **Funding**: This study was funded by Scientific direction and valorisation of AgroParisTech
521 (2015 incitative call, NUTRICAM project). It has benefited from a French State grant (LabEx
522 Saclay Plant Sciences-SPS, ref. ANR-10-LABX-0040-SPS), managed by the French National
523 Research Agency under an "Investments for the Future" program (ref. ANR-11-IDEX-0003-
524 02).

525

526 **Supporting information.**

527 Supplemental Table 1. Composition and nutritional values of the experimental diets.

528 Supplemental Table 2. SL composition of the camelina meals (nmol/g)

529 Supplemental Table 3. Body weight gain and food intake

530 Supplemental Figure 1. NH_2GIPCs and GlCers profiles in Camelina sativa seeds from the
531 commercial Céline cultivar (CamC24) and from the LOH2^{Y} line (CamC16).

532

533 **References.**

534 1. Alberti, K. G.; Eckel, R. H.; Grundy, S. M.; Zimmet, P. Z.; Cleeman, J. I.; Donato, K. A.; Fruchart,
535 J. C.; James, W. P.; Loria, C. M.; Smith, S. C., Jr., Harmonizing the metabolic syndrome: a joint interim
536 statement of the International Diabetes Federation Task Force on Epidemiology and Prevention;
537 National Heart, Lung, and Blood Institute; American Heart Association; World Heart Federation;
538 International Atherosclerosis Society; and International Association for the Study of Obesity.
539 *Circulation* **2009,** *120*, 1640-5.

2. Cornier, M. A.; Dabelea, D.; Hernandez, T. L.; Lindstrom, R. C.; Steig, A. J.; Stob, N. R.; Van Pelt, R. E.; Wang, H.; Eckel, R. H., The metabolic syndrome. *Endocr Rev* **2008,** *29*, 777-822.

3. Araujo, J. R.; Tomas, J.; Brenner, C.; Sansonetti, P. J., Impact of high-fat diet on the intestinal microbiota and small intestinal physiology before and after the onset of obesity. *Biochimie* **2017,** *141*, 97-106.

4. Dandona, P.; Ghanim, H.; Chaudhuri, A.; Dhindsa, S.; Kim, S. S., Macronutrient intake induces oxidative and inflammatory stress: potential relevance to atherosclerosis and insulin resistance. *Experimental & molecular medicine* **2010,** *42*, 245-53.

5. Tremaroli, V.; Backhed, F., Functional interactions between the gut microbiota and host metabolism. *Nature* **2012,** *489*, 242-9.

6. Ji, Y.; Sakata, Y.; Tso, P., Nutrient-induced inflammation in the intestine. *Curr Opin Clin Nutr Metab Care* **2011,** *14*, 315-21.

7. Cani, P. D.; Bibiloni, R.; Knauf, C.; Waget, A.; Neyrinck, A. M.; Delzenne, N. M.; Burcelin, R., Changes in gut microbiota control metabolic endotoxemia-induced inflammation in high-fat diet-induced obesity and diabetes in mice. *Diabetes* **2008,** *57*, 1470-81.

8. Minihane, A. M.; Vinoy, S.; Russell, W. R.; Baka, A.; Roche, H. M.; Tuohy, K. M.; Teeling, J. L.; Blaak, E. E.; Fenech, M.; Vauzour, D.; McArdle, H. J.; Kremer, B. H.; Sterkman, L.; Vafeiadou, K.; Benedetti, M. M.; Williams, C. M.; Calder, P. C., Low-grade inflammation, diet composition and health: current research evidence and its translation. *Br J Nutr* **2015,** *114*, 999-1012.

9. Nagpal, R.; Kumar, M.; Yadav, A. K.; Hemalatha, R.; Yadav, H.; Marotta, F.; Yamashiro, Y., Gut microbiota in health and disease: an overview focused on metabolic inflammation. *Beneficial microbes* **2016,** *7*, 181-94.

10. Berkey, R.; Bendigeri, D.; Xiao, S., Sphingolipids and plant defense/disease: the "death" connection and beyond. *Frontiers in plant science* **2012,** *3*, 68.

11. Lipina, C.; Hundal, H. S., Sphingolipids: agents provocateurs in the pathogenesis of insulin resistance. *Diabetologia* **2011,** *54*, 1596-607.

566 12. Langeveld, M.; Aerts, J. M., Glycosphingolipids and insulin resistance. *Prog Lipid Res* **2009,** *48*,
567 196-205.
568 13. Park, J. W.; Park, W. J.; Kuperman, Y.; Boura-Halfon, S.; Pewzner-Jung, Y.; Futerman, A. H.,
569 Ablation of very long acyl chain sphingolipids causes hepatic insulin resistance in mice due to altered
570 detergent-resistant membranes. *Hepatology* **2013,** *57*, 525-32.
571 14. Duivenvoorden, I.; Voshol, P. J.; Rensen, P. C.; van Duyvenvoorde, W.; Romijn, J. A.; Emeis, J.
572 J.; Havekes, L. M.; Nieuwenhuizen, W. F., Dietary sphingolipids lower plasma cholesterol and
573 triacylglycerol and prevent liver steatosis in APOE*3Leiden mice. *Am J Clin Nutr* **2006,** *84*, 312-21.
574 15. Snel, M.; Sleddering, M. A.; Pijl, H.; Nieuwenhuizen, W. F.; Frolich, M.; Havekes, L. M.; Romijn,
575 J. A.; Jazet, I. M., The effect of dietary phytosphingosine on cholesterol levels and insulin sensitivity in
576 subjects with the metabolic syndrome. *Eur J Clin Nutr* **2010,** *64*, 419-23.
577 16. Murakami, I.; Mitsutake, S.; Kobayashi, N.; Matsuda, J.; Suzuki, A.; Shigyo, T.; Igarashi, Y.,
578 Improved high-fat diet-induced glucose intolerance by an oral administration of phytosphingosine.
579 *Bioscience, biotechnology, and biochemistry* **2013,** *77*, 194-7.
580 17. Yunoki, K.; Renaguli, M.; Kinoshita, M.; Matsuyama, H.; Mawatari, S.; Fujino, T.; Kodama, Y.;
581 Sugiyama, M.; Ohnishi, M., Dietary sphingolipids ameliorate disorders of lipid metabolism in Zucker
582 fatty rats. *J Agric Food Chem* **2010,** *58*, 7030-5.
583 18. Zigmond, E.; Zangen, S. W.; Pappo, O.; Sklair-Levy, M.; Lalazar, G.; Zolotaryova, L.; Raz, I.; Ilan,
584 Y., Beta-glycosphingolipids improve glucose intolerance and hepatic steatosis of the Cohen diabetic
585 rat. *Am J Physiol Endocrinol Metab* **2009,** *296*, E72-8.
586 19. Lalazar, G.; Zigmond, E.; Weksler-Zangen, S.; Ben Ya'acov, A.; Sklair Levy, M.; Hemed, N.; Raz,
587 I.; Ilan, Y., Oral Administration of beta-Glucosylceramide for the Treatment of Insulin Resistance and
588 Nonalcoholic Steatohepatitis: Results of a Double-Blind, Placebo-Controlled Trial. *J Med Food* **2017**.
589 20. Zigmond, E.; Tayer-Shifman, O.; Lalazar, G.; Ben Ya'acov, A.; Weksler-Zangen, S.; Shasha, D.;
590 Sklair-Levy, M.; Zolotarov, L.; Shalev, Z.; Kalman, R.; Ziv, E.; Raz, I.; Ilan, Y., beta-glycosphingolipids

591 ameliorated non-alcoholic steatohepatitis in the Psammomys obesus model. *Journal of inflammation*
592 *research* **2014,** *7*, 151-8.
593 21. Norris, G. H.; Blesso, C. N., Dietary sphingolipids: potential for management of dyslipidemia
594 and nonalcoholic fatty liver disease. *Nutr Rev* **2017,** *75*, 274-285.
595 22. Zhang, W.; Moritoki, Y.; Tsuneyama, K.; Yang, G. X.; Ilan, Y.; Lian, Z. X.; Gershwin, M. E., Beta-
596 glucosylceramide ameliorates liver inflammation in murine autoimmune cholangitis. *Clinical and*
597 *experimental immunology* **2009,** *157*, 359-64.
598 23. Arai, K.; Mizobuchi, Y.; Tokuji, Y.; Aida, K.; Yamashita, S.; Ohnishi, M.; Kinoshita, M., Effects of
599 Dietary Plant-Origin Glucosylceramide on Bowel Inflammation in DSS-Treated Mice. *J Oleo Sci* **2015,**
600 *64*, 737-42.
601 24. Bryan, P. F.; Karla, C.; Edgar Alejandro, M. T.; Sara Elva, E. P.; Gemma, F.; Luz, C.,
602 Sphingolipids as Mediators in the Crosstalk between Microbiota and Intestinal Cells: Implications for
603 Inflammatory Bowel Disease. *Mediators of inflammation* **2016,** *2016*, 9890141.
604 25. Camp, E. R.; Patterson, L. D.; Kester, M.; Voelkel-Johnson, C., Therapeutic implications of
605 bioactive sphingolipids: A focus on colorectal cancer. *Cancer biology & therapy* **2017,** *18*, 640-650.
606 26. Duan, J.; Sugawara, T.; Sakai, S.; Aida, K.; Hirata, T., Oral glucosylceramide reduces 2,4-
607 dinitrofluorobenzene induced inflammatory response in mice by reducing TNF-alpha levels and
608 leukocyte infiltration. *Lipids* **2011,** *46*, 505-12.
609 27. Mazzei, J. C.; Zhou, H.; Brayfield, B. P.; Hontecillas, R.; Bassaganya-Riera, J.; Schmelz, E. M.,
610 Suppression of intestinal inflammation and inflammation-driven colon cancer in mice by dietary
611 sphingomyelin: importance of peroxisome proliferator-activated receptor gamma expression. *J Nutr*
612 *Biochem* **2011,** *22*, 1160-71.
613 28. Yamashita, S.; Sakurai, R.; Hishiki, K.; Aida, K.; Kinoshita, M., Effects of Dietary Plant-origin
614 Glucosylceramide on Colon Cytokine Contents in DMH-treated Mice. *J Oleo Sci* **2017,** *66*, 157-160.
615 29. Tellier, F.; Maia-Grondard, A.; Schmitz-Afonso, I.; Faure, J. D., Comparative plant
616 sphingolipidomic reveals specific lipids in seeds and oil. *Phytochemistry* **2014,** *103*, 50-8.

30. Julie-Galau, S.; Bellec, Y.; Faure, J. D.; Tepfer, M., Evaluation of the potential for interspecific hybridization between Camelina sativa and related wild Brassicaceae in anticipation of field trials of GM camelina. *Transgenic research* **2014,** *23*, 67-74.

31. Morineau, C.; Bellec, Y.; Tellier, F.; Gissot, L.; Kelemen, Z.; Nogue, F.; Faure, J. D., Selective gene dosage by CRISPR-Cas9 genome editing in hexaploid Camelina sativa. *Plant biotechnology journal* **2017,** *15*, 729-739.

32. de Andrade, P. V.; Schmidely, P., Effect of duodenal infusion of trans10,cis12-CLA on milk performance and milk fatty acid profile in dairy goats fed high or low concentrate diet in combination with rolled canola seed. *Reprod Nutr Dev* **2006,** *46*, 31-48.

33. Beaumont, M.; Andriamihaja, M.; Armand, L.; Grauso, M.; Jaffrezic, F.; Laloe, D.; Moroldo, M.; Davila, A. M.; Tome, D.; Blachier, F.; Lan, A., Epithelial response to a high-protein diet in rat colon. *BMC Genomics* **2017,** *18*, 116.

34. Fossati, P.; Prencipe, L., Serum triglycerides determined colorimetrically with an enzyme that produces hydrogen peroxide. *Clin Chem* **1982,** *28*, 2077-80.

35. Takayama, M.; Itoh, S.; Nagasaki, T.; Tanimizu, I., A new enzymatic method for determination of serum choline-containing phospholipids. *Clin Chim Acta* **1977,** *79*, 93-8.

36. Markham, J. E.; Jaworski, J. G., Rapid measurement of sphingolipids from Arabidopsis thaliana by reversed-phase high-performance liquid chromatography coupled to electrospray ionization tandem mass spectrometry. *Rapid communications in mass spectrometry : RCM* **2007,** *21*, 1304-14.

37. Fujii, A.; Manabe, Y.; Aida, K.; Tsuduki, T.; Hirata, T.; Sugawara, T., Selective Absorption of Dietary Sphingoid Bases from the Intestine via Efflux by P-Glycoprotein in Rats. *J Nutr Sci Vitaminol (Tokyo)* **2017,** *63*, 44-50.

38. Ishikawa, J.; Takada, S.; Hashizume, K.; Takagi, Y.; Hotta, M.; Masukawa, Y.; Kitahara, T.; Mizutani, Y.; Igarashi, Y., Dietary glucosylceramide is absorbed into the lymph and increases levels of epidermal sphingolipids. *Journal of dermatological science* **2009,** *56*, 220-2.

643 39. Sugawara, T.; Kinoshita, M.; Ohnishi, M.; Nagata, J.; Saito, M., Digestion of maize
644 sphingolipids in rats and uptake of sphingadienine by Caco-2 cells. *J Nutr* **2003,** *133*, 2777-82.
645 40. Sugawara, T.; Tsuduki, T.; Yano, S.; Hirose, M.; Duan, J.; Aida, K.; Ikeda, I.; Hirata, T., Intestinal
646 absorption of dietary maize glucosylceramide in lymphatic duct cannulated rats. *J Lipid Res* **2010,** *51*,
647 1761-9.
648 41. Hermier, D.; Guelzim, N.; Martin, P. G.; Huneau, J. F.; Mathe, V.; Quignard-Boulange, A.;
649 Lasserre, F.; Mariotti, F., NO synthesis from arginine is favored by alpha-linolenic acid in mice fed a
650 high-fat diet. *Amino Acids* **2016,** *48*, 2157-68.
651 42. Lam, Y. Y.; Ha, C. W.; Hoffmann, J. M.; Oscarsson, J.; Dinudom, A.; Mather, T. J.; Cook, D. I.;
652 Hunt, N. H.; Caterson, I. D.; Holmes, A. J.; Storlien, L. H., Effects of dietary fat profile on gut
653 permeability and microbiota and their relationships with metabolic changes in mice. *Obesity (Silver*
654 *Spring)* **2015,** *23*, 1429-39.
655 43. Chung, R. W.; Kamili, A.; Tandy, S.; Weir, J. M.; Gaire, R.; Wong, G.; Meikle, P. J.; Cohn, J. S.;
656 Rye, K. A., Dietary sphingomyelin lowers hepatic lipid levels and inhibits intestinal cholesterol
657 absorption in high-fat-fed mice. *PLoS One* **2013,** *8*, e55949.
658 44. Lalazar, G.; Zigmond, E.; Weksler-Zangen, S.; Ya'acov, A. B.; Levy, M. S.; Hemed, N.; Raz, I.;
659 Ilan, Y., Oral Administration of beta-Glucosylceramide for the Treatment of Insulin Resistance and
660 Nonalcoholic Steatohepatitis: Results of a Double-Blind, Placebo-Controlled Trial. *J Med Food* **2017,**
661 *20*, 458-464.
662 45. Milard, M.; Laugerette, F.; Durand, A.; Buisson, C.; Meugnier, E.; Loizon, E.; Louche-Pelissier,
663 C.; Sauvinet, V.; Garnier, L.; Viel, S.; Bertrand, K.; Joffre, F.; Cheillan, D.; Humbert, L.; Rainteau, D.;
664 Plaisancie, P.; Bindels, L. B.; Neyrinck, A. M.; Delzenne, N. M.; Michalski, M. C., Milk Polar Lipids in a
665 High-Fat Diet Can Prevent Body Weight Gain: Modulated Abundance of Gut Bacteria in Relation with
666 Fecal Loss of Specific Fatty Acids. *Mol Nutr Food Res* **2019,** *63*, e1801078.
667 46. Norris, G. H.; Jiang, C.; Ryan, J.; Porter, C. M.; Blesso, C. N., Milk sphingomyelin improves lipid
668 metabolism and alters gut microbiota in high fat diet-fed mice. *J Nutr Biochem* **2016,** *30*, 93-101.

669 47. Chaturvedi, S.; Bhattacharya, A.; Khare, S. K.; Kaushik, G., Camelina sativa: An Emerging
670 Biofuel Crop. In *Handbook of Environmental Materials Management*, Hussain, C. M., Ed. Springer
671 International Publishing: Cham, 2018; pp 1-38.
672 48. Smit, M. N.; Beltranena, E., Effects of feeding camelina cake to weaned pigs on safety,
673 growth performance, and fatty acid composition of pork. *Journal of animal science* **2017,** *95*, 2496-
674 2508.
675 49. Norris, G. H.; Blesso, C. N., Dietary and Endogenous Sphingolipid Metabolism in Chronic
676 Inflammation. *Nutrients* **2017,** *9*.
677 50. Muller, V. M.; Zietek, T.; Rohm, F.; Fiamoncini, J.; Lagkouvardos, I.; Haller, D.; Clavel, T.;
678 Daniel, H., Gut barrier impairment by high-fat diet in mice depends on housing conditions. *Mol Nutr*
679 *Food Res* **2016,** *60*, 897-908.
680 51. Tomas, J.; Mulet, C.; Saffarian, A.; Cavin, J. B.; Ducroc, R.; Regnault, B.; Kun Tan, C.; Duszka,
681 K.; Burcelin, R.; Wahli, W.; Sansonetti, P. J.; Pedron, T., High-fat diet modifies the PPAR-gamma
682 pathway leading to disruption of microbial and physiological ecosystem in murine small intestine.
683 *Proc Natl Acad Sci U S A* **2016,** *113*, E5934-E5943.

684

685

686

Table 1. SL composition of the experimental diets (nmol/g).

	NC	HC-Con	HC-CamC24	HC-CamC16
Total Cer	125	54	61	70
C16-Cer	11.4	8.36	9.39	14.7
C24-Cer	43.7	14.3	16.6	17.5
Total hCer	107	34	44	53
C16-hCer	4.99	5.61	5.84	10.9
C24-hCer	45.2	13.0	18.1	19.7
Total GluCer	20	0.44	10.6	7.6
C16-GluCer	6.26	0.14	1.53	4.3
C24-GluCer	8.30	0.20	7.08	2.4
Total NH_2GIPC	222	5.31	444	463
C16-NH_2GIPC	0.82	0.38	6.71	421
C24-NH_2GIPC	98.9	2.61	363	33
Total SL	473	94.0	560	593
C16-SL	23.4	14.3	23.5	450
C24-SL	194	30.0	404	72.6
Total NH_2GIPC (% of total SL)	46.9	5.6	79.3	78.1
C16-NH_2GIPC (% of total NH_2GIPC)	0.37	7.16	1.51	90.9
C24-NH_2GIPC (% of total NH_2GIPC)	44.5	49.2	81.8	7.1

NC, normo-caloric; HC, hyper-caloric; Con, control; CamC24, camelina meal C24 (from the commercial Céline cultivar rich in C24 fatty acids); CamC16, camelina meal C16 (from the experimental LOH2 cultivar rich in C16 fatty acids); hCer, hydroxyceramide; GluCer, glucosyl-ceramide; NH_2GIPC, aminoglycosyl-inositol-phosphoryl-ceramide.

711 **Table 2. Body composition after 3 and 5 weeks on the experimental diets**

	NC	HC-Con	HC-CamC24	HC-CamC16	*P* ANOVA
After 3 weeks					
Body weight (fed state, g)	25.6±2.0^{a}	29.9±2.4^{b}	27.1±1.4^{a}	27.0±1.0^{a}	0.0013
Lean body mass (g)	21.2±1.5^{a}	21.0±0.9^{a}	20.0±1.1^{a}	20.5±0.7^{a}	0.1086
Fat body mass (g)	4.28±0.79^{a}	8.31±1.92^{c}	6.69±1.72^{bc}	6.19±1.07^{ab}	0.0006
Fat body mass (% body weight)	16.7±2.4^{a}	28.1±4.8^{b}	24.9±5.2^{b}	23.1±3.2^{b}	0.0004
After 5 weeks					
Body weight (fasted state, g)	26.7±2.5^{a}	31.5±4.1^{b}	28.6±0.5^{ab}	28.6±1.3^{ab}	0.0148
EAT (mg)	558±117^{a}	1446±520^{b}	911±199^{a}	946±186^{a}	0.0003
EAT (% body weight)	2.08±0.36^{a}	4.48±1.18^{c}	3.19±0.60^{b}	3.29±0.52^{b}	0.0002
Liver (g)	1.18±0.15^{a}	1.16±0.16^{a}	1.07±0.20^{a}	1.05±0.17^{a}	0.4780
Small intestine (mg)	947±96^{a}	836±91^{a}	830±60^{a}	862±84^{a}	0.0546
Caecum (mg)	109±23^{a}	58±33^{b}	69±18^{b}	67±13^{b}	0.0002
Caecum content (mg)	301±76^{a}	157±41^{b}	164±53^{b}	185±31^{b}	<0.0001
Colon (mg)	193±19^{a}	139±25^{b}	132±15^{b}	131±29^{b}	<0.0001
Colon content (mg)	115±17^{a}	79±21^{a}	91±28^{a}	101±34^{a}	0.0968

712 Values are means ± standard deviations for 6 and 9 mice in the NC and the three HC- groups,
713 respectively. Mean values within a row, not sharing a same superscript letter, were
714 significantly different at $P<0.05$.

715 NC, normo-caloric; HC, hyper-caloric; Con, control; CamC24, camelina meal C24 (from the
716 commercial Céline cultivar rich in C24 fatty acids); CamC16, camelina meal C16 (from the
717 experimental LOH2 cultivar rich in C16 fatty acids); EAT, epididymal adipose tissue.

718 **Table 3. Blood markers associated with a MetS after 3 weeks (during an OGTT) and 5**

719 **weeks on the experimental diets.**

	NC	HC-Con	HC-CamC24	HC-CamC16	*P* ANOVA
3 weeks					
Glucose t0 (g/L)	1.22±0.10^{a}	1.59±0.13^{b}	1.52±0.14^{b}	1.51±0.13^{b}	<0.0001
Insulin t0 (µg/L)	0.67±0.33^{a}	1.37±0.38^{b}	0.90±0.42^{ab}	0.78±0.33^{a}	0.0035
HOMA-IR index	5.63±2.48^{a}	15.60±5.03^{b}	9.73±4.36^{a}	8.33±3.54^{a}	0.0004
Δ glucose (t30-t0 g/L)	0.59±0.17^{a}	1.41±0.50^{b}	1.22±0.78^{ab}	0.91±0.32^{ab}	0.0261
5 weeks					
Glucose (g/L)	1.18±0.17^{a}	1.60±0.17^{b}	1.58±0.14^{b}	1.55±0.14^{b}	<0.0001
Triglyceride (g/L)	0.69±0.18^{a}	0.60±10^{a}	0.35±0.04^{b}	0.38±0.09^{b}	<0.0001
Cholesterol (g/L)	1.01±0.18 ^{a}	1.55±0.47^{ab}	1.73±0.32^{b}	1.74±0.19^{b}	0.0088

720

721 Values are means ± standard deviations for 6 and 9 mice in the NC and the three HC- groups,

722 respectively. Mean values within a row, not sharing a same superscript letter, were

723 significantly different at $P<0.05$.

724 NC, normo-caloric; HC, hyper-caloric; Con, control; CamC24, camelina meal C24 (from the

725 commercial Céline cultivar rich in C24 fatty acids); CamC16, camelina meal C16 (from the

726 experimental LOH2 cultivar rich in C16 fatty acids).

727 HOMA-IR: homeostasis model assessment of insulin resistance

728

729 **Table 4. Relative gene expression level of some markers of low-grade inflammation.**

730

	NC	HC-Con	HC-CamC24	HC-CamC16	*P* ANOVA
EAT					
Mcp-1	1.19±0.72[a]	3.55±2.07[b]	2.79±1.10[ab]	2.08±0.77[ab]	0.0168
Pai-1	1.24±0.81[a]	2.67±1.02[ab]	4.12±1.64[b]	3.17±1.28[b]	0.0021
Colon					
Il-1β	1.03±0.25[a]	2.03±1.02[b]	1.60±0.39[ab]	1.58±0.44[ab]	0.0707

731

732 Values are means ± standard deviations for 6 and 8-9 mice in the NC and the three HC-
733 groups, respectively. They were calculated according to the $2^{-\Delta\Delta Ct}$, where ΔCt = (Ct target
734 gene - Ct HPRT) normalized to the NC group. Mean values within a row, not sharing a same
735 superscript letter, were significantly different at $P<0.05$.

736 NC, normo-caloric; HC, hyper-caloric; Con, control; CamC24, camelina meal C24 (from the
737 commercial Céline cultivar rich in C24 fatty acids); CamC16, camelina meal C16 (from the
738 experimental LOH2 cultivar rich in C16 fatty acids).

739

740 **Table 5. Electrical measurement of colon epithelium parameters in Ussing chambers.**

741

	NC	HC-Con	HC-CamC24	HC-CamC16	*P* ANOVA
V_t (mV)	-2.78±0.15^{a}	-8.45±0.83^{b}	-9.08±1.32^{b}	-5.90±1.30^{c}	<0.0001
I_{sc}(µA/cm^2)	59±10^{a}	166±17^{b}	149±14^{b}	142±3^{b}	<0.0001
G_t (mS/cm^2)	16.8±2.2^{ab}	16.5±1.8^{ab}	14.0±2.4^{a}	20.1± 3.3^{b}	0.0396

742

743 Measures were acquired after 45-minutes epithelium equilibration in recording buffer. V_t,
744 trans-epithelial voltage; I_{sc}, short-circuit current; G_t, trans-epithelial electrical conductance.
745 Values are means ± standard deviations for 3-4 mice in each group.
746 Mean values within a row, not sharing a same superscript letter, were significantly different
747 at P<0.05.
748 NC, normo-caloric; HC, hyper-caloric; Con, control; CamC24, camelina meal C24 (from the
749 commercial Céline cultivar rich in C24 fatty acids); CamC16, camelina meal C16 (from the
750 experimental LOH2 cultivar rich in C16 fatty acids).

751

Table 6. Intake, excretion, and apparent digestibility of NH_2GIPC after 4 weeks on the experimental diets.

	NC	HC-Con	HC-CamC24	HC-CamC16	*P* ANOVA
NH_2GIPC Intake (nmol/d)	784±36^{b}	17.7±1.5^{c}	1209±186^{a}	1358±195^{a}	<0.0001
NH_2-GIPC Excretion (nmol/d)	43.7±10.5^{c}	2.45±0.84^{c}	113±33^{b}	278±48^{a}	<0.0001
NH_2GIPC Excretion (intake %)	5.74±1.49^{c}	13.73±4.30^{b}	9.40±2.58^{c}	20.33±2.61^{a}	<0.0001
Apparent digestibility (intake %)	94.3±1.5^{a}	86.3±2.6^{b}	90.6+2.6^{ab}	79.7±2.6^{c}	<0.0001

Values are means ± standard deviations for 6 and 9 mice in the NC and the three HC- groups, respectively. Mean values within a row, not sharing a same superscript letter, were significantly different at $P<0.05$.

NC, normo-caloric; HC, hyper-caloric; Con, control; CamC24, camelina meal C24 (from the commercial Céline cultivar rich in C24 fatty acids); CamC16, camelina meal C16 (from the experimental LOH2 cultivar rich in C16 fatty acids).

761 **Table 7. Sphingolipid levels in the jejunum and colon (nmol/g).**

762

	NC	HC-Con	HC-CamC24	HC-CamC16	*P* ANOVA
Jejunum					
C16 GluCer	0.025 ± 0.021^{ab}	nd	0.009 ± 0.008^{b}	0.027 ± 0.016^{a}	0.0004
C24-GluCer	0.499 ± 0.295^{a}	0.108 ± 0.040^{b}	0.333 ± 0.150^{a}	0.289 ± 0.108^{ab}	0.0006
C16-NH_2GIPC	nd	nd	0.248 ± 0.122^{b}	11.683 ± 2.085^{a}	<0.0001
C24-NH_2GIPC	0.671 ± 0.231^{b}	nd	5.799 ± 1.609^{a}	0.481 ± 0.138^{b}	<0.0001
Colon					
C16-GluCer	nd	nd	nd	nd	-
C24-GluCer	0.151 ± 0.028^{a}	0.081 ± 0.044^{a}	0.125 ± 0.036^{a}	0.118 ± 0.069^{a}	0.0661
C16-NH_2GIPC	nd	nd	nd	1.901 ± 0.625	<0.0001
C24-NH_2GIPC	0.382 ± 0.214^{a}	nd	0.279 ± 0.072^{a}	0.123 ± 0.056^{b}	<0.0001

763

764 Values are means ± standard deviations for 6 and 9 mice in the NC and the three HC- groups,
765 respectively. Mean values within a row, not sharing a same superscript letter, were
766 significantly different at $P<0.05$; nd, not dectected.

767 NC, normo-caloric; HC, hyper-caloric; Con, control; CamC24, camelina meal C24 (from the
768 commercial Céline cultivar rich in C24 fatty acids); CamC16, camelina meal C16 (from the
769 experimental LOH2 cultivar rich in C16 fatty acids).

770

771

772 **Figure 1. Body weight curve and body weight gain upon 5 week feeding with the**

773 **experimental diets.**

	NC	HC-Con	HC-CamC24	HC-CamC16	*P* value
Weight gain (g)	3.47±1.06[b]	8.78±2.98[a]	5.21±1.24[b]	5.08±1.07[b]	<0.0001

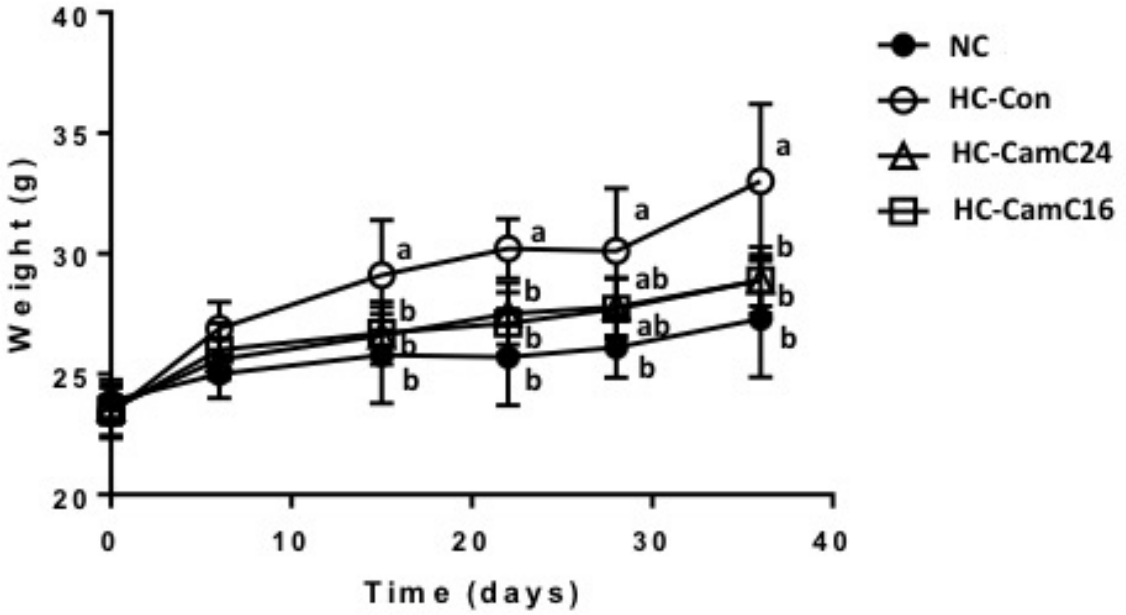

774

775

Figure 2. Plasma kinetics of glucose and insulin during an OGTT after 3 weeks on the experimental diets.

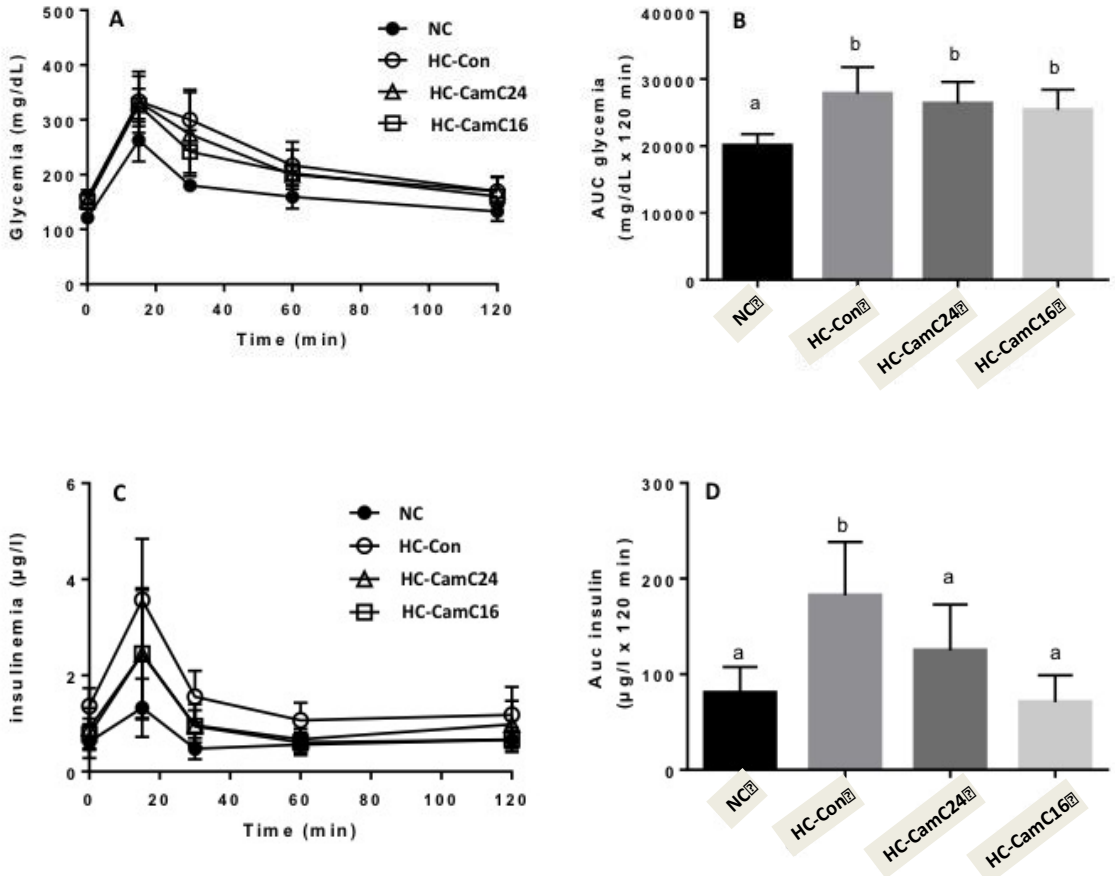

Legend to Figures.

Figure 1. Body weight curve.

Body weight (g) was measured longitudinally in the fed state for 37d. At d0, after they were acclimated to local conditions for 1 week, mice that have been given progressively the HC-Con diet during this 1st week, were switched to the HC-Con, HC-CamC24 and HC-CamC16 according to their experimental group.

Values are means ± standard deviations for 6 and 9 mice in the NC and the three HC- groups, respectively.

NC, normo-caloric; HC, hyper-caloric; Con, control; CamC24, camelina meal C24 (from the commercial Céline cultivar rich in C24 fatty acids); CamC16, camelina meal C16 (from the experimental LOH2 cultivar rich in C16 fatty acids).

Figure 2. Plasma kinetics of glucose and insulin during an OGTT after 3 weeks on the experimental diets.

Glycemia (Panel A) and insulinemia (Panel B) have been measured for 120 min and their respective area under the curve (AUC) were calculated over the same period of time (Panels B and D). Values are means ± standard deviations for 6 and 9 mice in the NC and the three HC- groups, respectively. Mean AUC values not sharing a same superscript letter, were significantly different at $P<0.05$.

804 NC, normo-caloric; HC, hyper-caloric; Con, control; CamC24, camelina meal C24 (from the
805 commercial Céline cultivar rich in C24 fatty acids); CamC16, camelina meal C16 (from the
806 experimental LOH2 cultivar rich in C16 fatty acids).
807
808
809
810
811
812